Supplementary information

Metabolism in action: stable isotope probing using vibrational spectroscopy and SIMS reveals kinetic and metabolic flux of key substrates

Malama Chisanga,[a,b] Howbeer Muhamadali,[c] Danielle Mcdougall,[d] Yun Xu,[c] Nicholas Lockyer,[d] and Royston Goodacre[*c]

[a]School of Chemistry, Manchester Institute of Biotechnology, University of Manchester, Manchester, UK, M1 7DN

[b]School of Mathematics and Natural Sciences, Department of Chemistry, Copperbelt University, Kitwe, Zambia

[c]Department of Biochemistry, Institute of Integrative Biology, University of Liverpool, Liverpool, UK, L69 7ZB

[d]School of Chemistry, Photon Science Institute, University of Manchester, Manchester, UK, M13 9PL

[*]**Corresponding author:**
Royston Goodacre, E-mail: roy.goodacre@liverpool.ac.uk, Tel: 0151 795 7689

EXPERIMENTAL METHODS

Raman spectroscopic analysis for kinetics measurements and phenol degradation study

Prior to Raman measurements, 2 µL of each of all cell samples were spotted on to clean and dry calcium fluoride (CaF_2) discs and dried for 30 min in a desiccator at room temperature. Raman spectra were recorded using an InVia confocal Raman spectrometer (Renishaw Plc., Gloucestershire, UK) equipped with a 785 nm diode near infrared laser with laser power on the sample adjusted to ~30 mW. The Raman instrument was calibrated with the phonon band of Si wafer focused under 50× objective (NA = 0.9) and collected as a static spectrum centered at 520 cm^{-1}. Raman spectra with a spectral resolution of 6 cm^{-1} were measured using a grating of 600 lines/mm and exposure time of 10 s with three spectral accumulations. Three spectra were acquired from different positions of each sample spot to account for batch to batch variations within each experimental condition.

Supplementary information

FT-IR spectroscopic analysis for kinetics measurements of ^{13}C incorporation by *E. coli*

Sample aliquots (20 μL) of washed and normalised *E. coli* were spotted onto a 96-well Si plate and dried in a 55°C oven. FT-IR spectra were obtained in transmission mode, on a Bruker Equinox 55 infrared spectrophotometer equipped with a HTX™ module (Bruker Optics Ltd, Coventry, UK). To improve the signal-to-noise ratio, 64 spectral scans were co-added for each sample between 4000-600 cm^{-1} at a spectral resolution of 4 cm^{-1}.

Data processing and analysis

All statistical analysis was carried out on MATLAB version 2015a (The MathWorks Inc., Natwick, US). All collected Raman and FT-IR spectra were subjected to baseline correction using asymmetric least squares (AsLS)[1], before multivariate analysis. Baseline corrected Raman and FT-IR data were scaled using autoscaling[2], and extended multiplicative signal correction (EMSC)[3], respectively. For all FT-IR data, the CO_2 signals in the 2400-2275 cm^{-1} range were removed and filled with a linear trend prior to EMSC scaling.

Principal component analysis (PCA) was employed as an unsupervised algorithm to reduce data dimensionality for both Raman and FT-IR data. PCA is exploratory by nature[4], so it was employed to identify natural differences and similarities, which in this case were sampling time and concentration of $^{12}C/^{13}C$ isotopes within the cells[5].

Table S1. Major Raman spectral band redshifts (-Δ cm^{-1}) due to ^{13}C isotope assimilation by *E. coli*.

Standard Raman	^{13}C labelled	Band assignment

Supplementary information

position (cm^{-1})	cells (Δ cm^{-1})	
1654	-34	Amide I (C=O and C–N stretch, N–H bend)
1575	-47	Guanine, adenine (ring stretch)
1338	-24	Adenine (ring stretch)
1245	-10	Amide III (C–N stretch, N–H bend)
1096	-28	Glycosidic link (C–O–C stretch, C–C skeletal)
1002	-37	Phenylalanine (ring breath)
828	-28	Tyrosine (exposed ring breath)
783	-15	Cytosine, uracil (ring breath)
642	-15	Tyrosine (skeletal)

Table S2. Major FT-IR spectral band redshifts (-Δ cm^{-1}) due to ^{13}C isotope incorporation by *E. coli.*

Standard FT-IR position (cm^{-1})	^{13}C labelled cells (Δ cm^{-1})	Band assignment
2925	-9	Lipids (CH_2 asymmetric stretch)
2849	-11	Lipids (CH_2 symmetric stretch)
1654	-38	Amide I (C=O and C–N stretch, N–H bend)
1544	-13	Amide II (C–N stretch, N–H bend)
1400	-27	Amino acids, lipids (COO^- stretch)
1244	-8	Amide III (N–H in-plane bend, C–N stretch)

Supplementary information

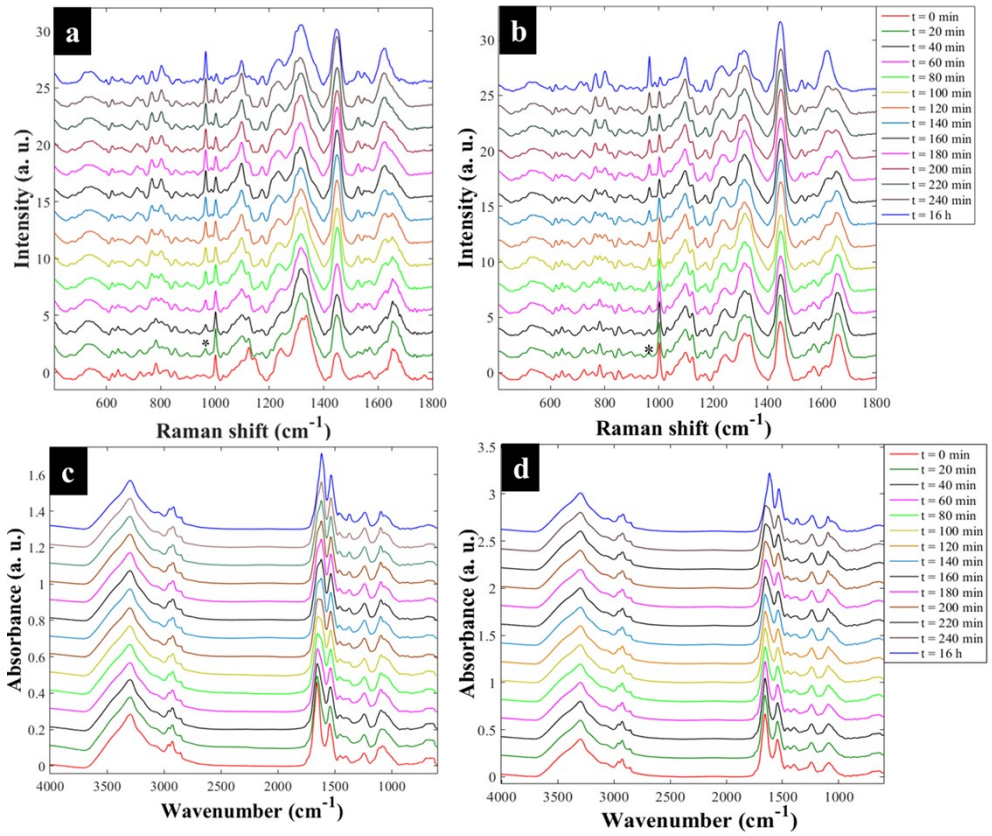

Figure S1. Averaged Raman (**a, b**) and FT-IR (**c, d**) spectra showing kinetic incorporation of ^{13}C in *E. coli* during growth on minimal medium supplemented with 5 g/L ^{13}C-glucose at 37 and 25°C, respectively. All spectra were measured from cells harvested at 20 min intervals from 0 to 4 h, and then after 16 h. Asterisks (*) on Raman spectra in **(a and b)** denotes clear band redshift detected at 965 cm^{-1} after 20 min of cell growth at 37°C, which occurs later in cells grown at 25°C **(b)**. The redshift in amide I for FT-IR in **(c)** was clearer when only cells collected at 0 and 20 min were considered as shown on Figure S3. All spectra are overlaid for clear visualisation of band redshifts.

Supplementary information

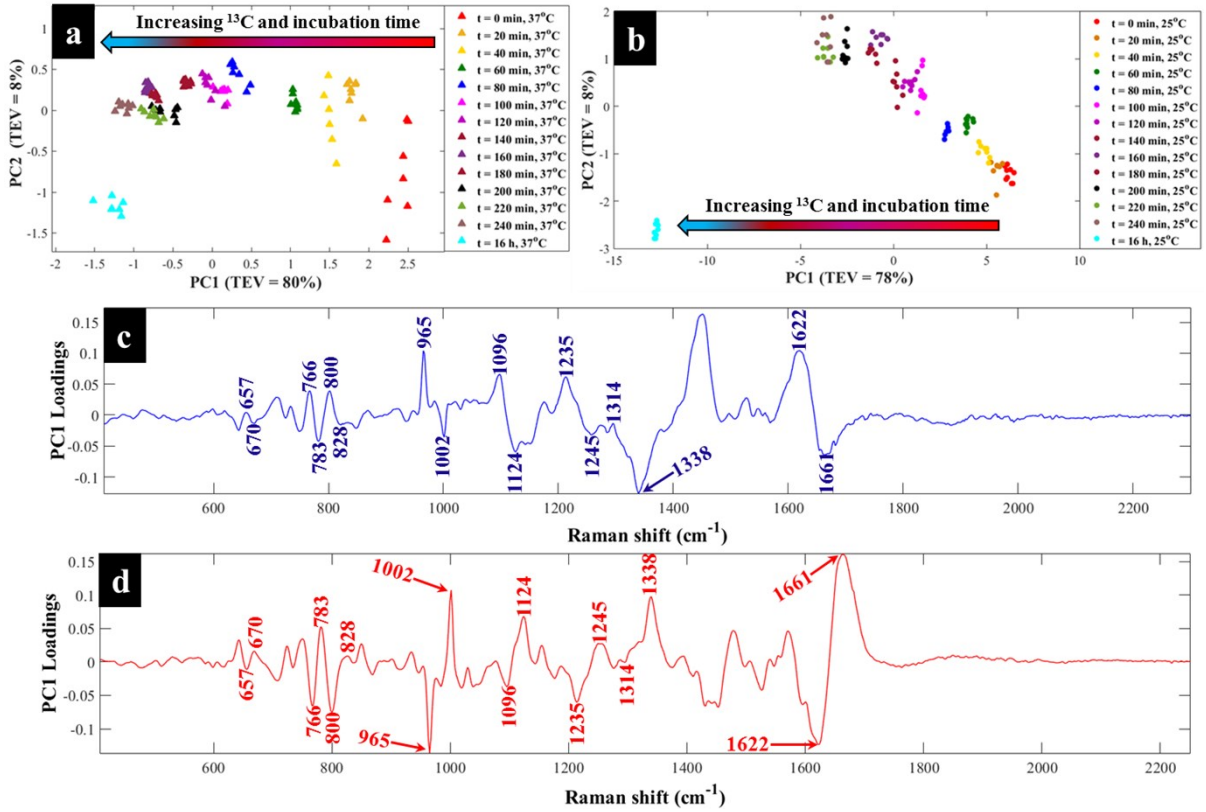

Figure S2. PCA scores and PC1 loadings plots of Raman spectra from *E. coli* during incubation on minimal medium supplemented with 5 g/L ^{13}C-glucose at 37°C **(a, c)** and 25°C **(b, d)**. PC loadings **(c, d)** highlight major bands (annotated by wavenumbers above bands) affected by isotope assimilation, and hence responsible for the sampling time and ^{13}C concentration-dependent clustering in PCA **(a, b)**; where TEV = total explained variance by that PC. The arrows on PCA **(a, b)**, and wavenumbers on PC loadings **(c, d)** plots are included for clarity.

Supplementary information

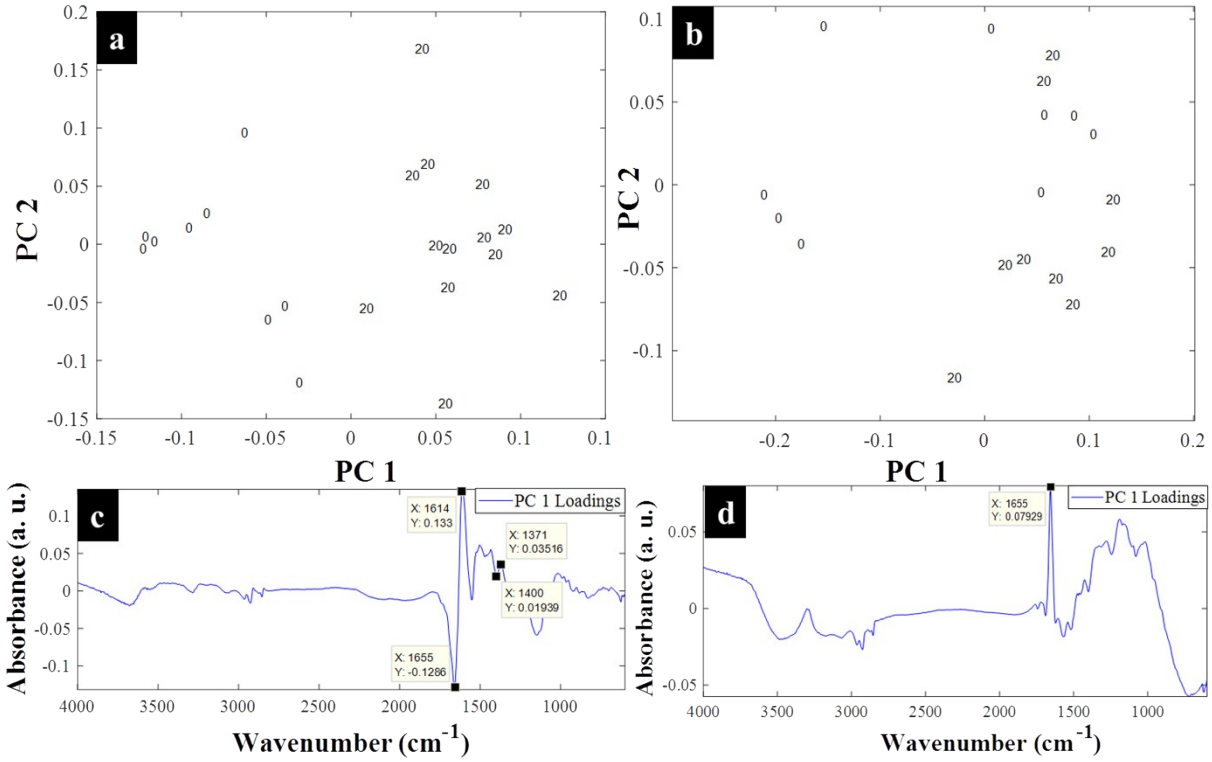

Figure S3. PCA scores **(a, b)** and loadings **(c, d)** plots of FT-IR data for *E. coli* cultivated on minimal medium supplemented with 5 g/L ^{13}C-glucose for 0 and 20 min at 37°C **(a, c)** and 25°C **(b, d)**, showing rapid incorporation of ^{13}C via redshifts for amide I (1655 to 1614 cm^{-1}) and lipids (1400 to 1371 cm^{-1}) at 37°C **(a, c)**. The numbers on **(a, b)** represent sampling points, i.e. 0 and 20 min were the first and second time points, respectively, whilst the ones on **(c, d)** are wavenumbers for redshifted FT-IR bands. No spectral redshifts were detectable on the FT-IR spectrum of *E. coli* cells grown at 25°C **(b, d)**, since the majority of cells were not sufficiently labelled with ^{13}C isotope.

Supplementary information

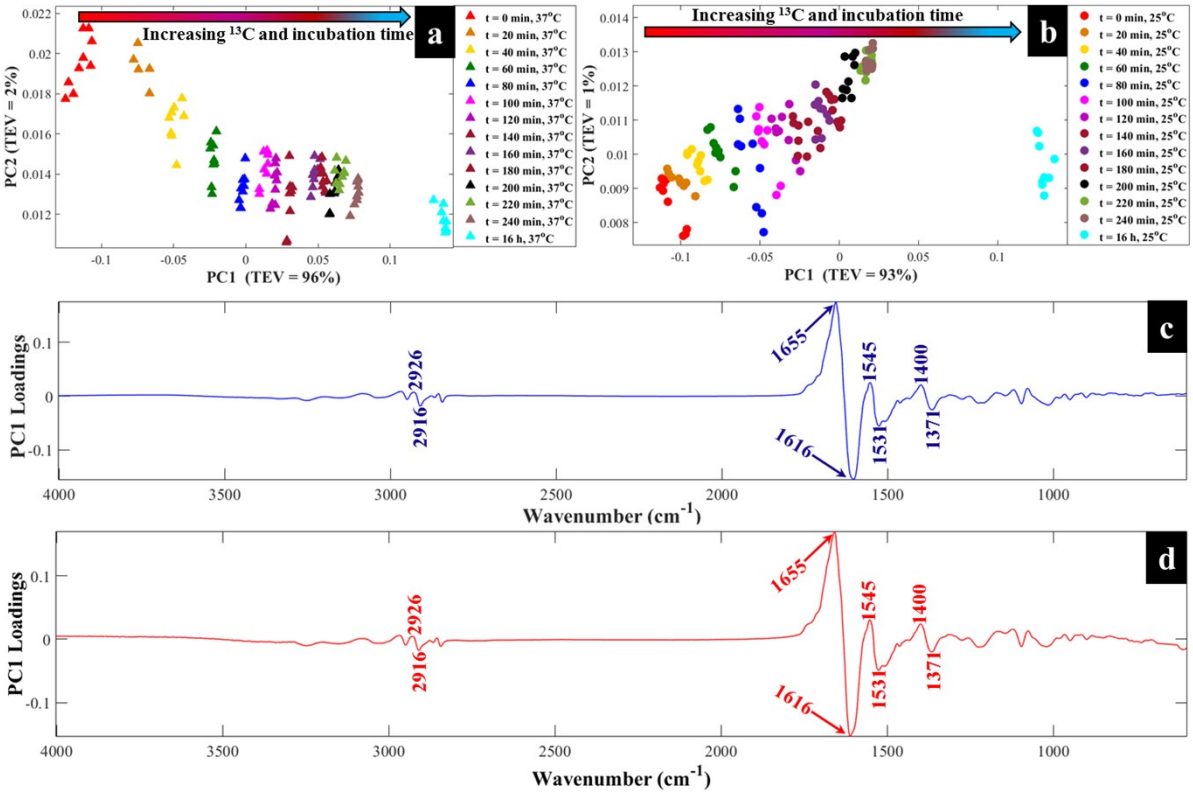

Figure S4. PCA scores and PC1 explanatory spectral variables (loadings) of FT-IR spectra from *E. coli* cells during growth in ^{13}C-glucose (5 g/L) minimal medium at 37°C (**a, c**) and 25°C **(b, d)** incubation conditions. PC1 loadings **(c, d)** for both incubation temperatures reveal the amide I (1655 cm^{-1}) and amide II (1545 cm^{-1}) as the main FT-IR modes displaying major band redshifts due to ^{13}C assimilation by cells, and thus associated with clustering patterns observed in PCA scores **(a, b)**. The arrows on PCA **(a, b)**, and wavenumbers on PC loadings **(c, d)** are included for clarity; note that PC1 shows the majority of the TEV and very little variance is explained in PC2 which is why we concentrate on the first PC.

Supplementary information

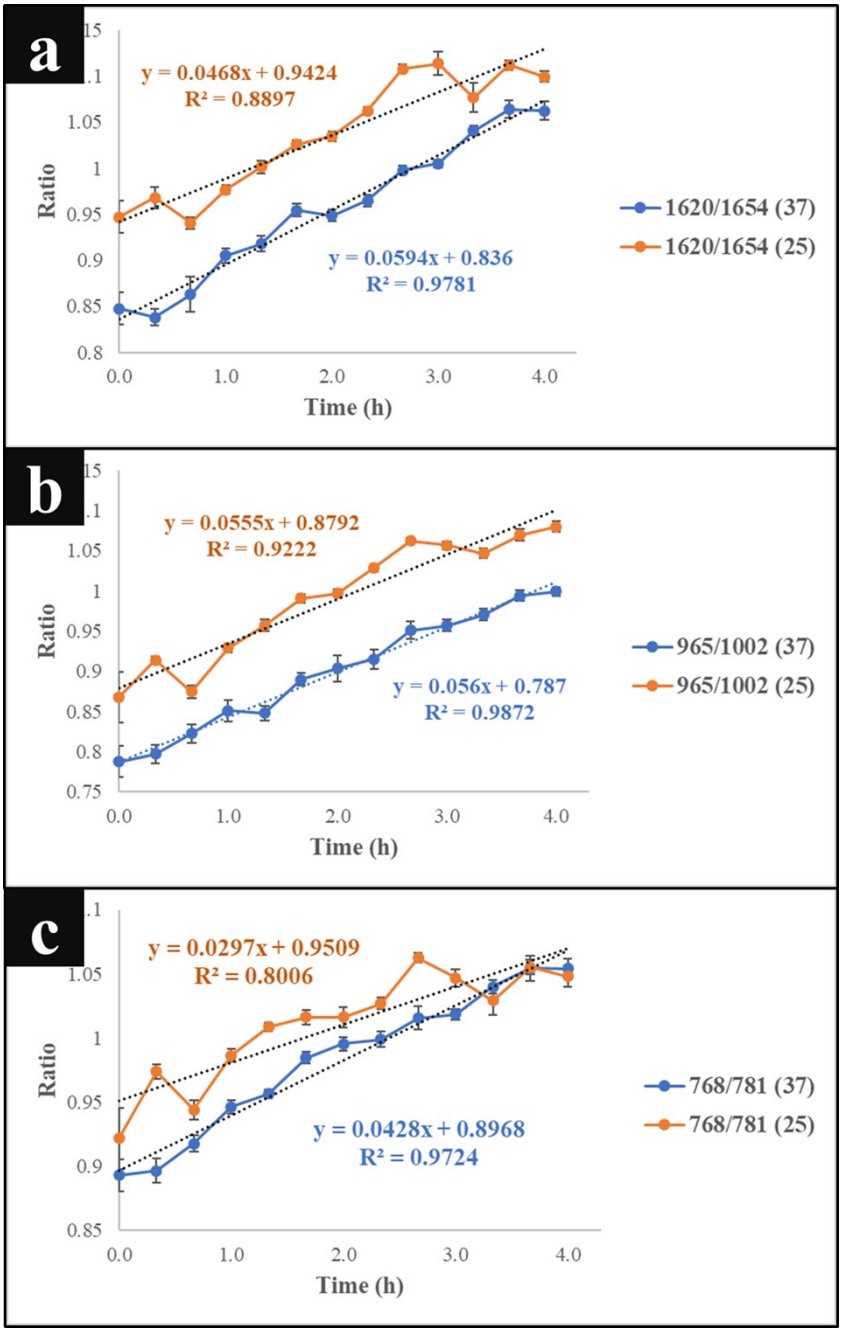

Figure S5. Intensity ratio plots for $^{13}C/^{12}C$ of different Raman bands representing **(a)** amide I, **(b)** phenylalanine and **(c)** DNA bases, indicating the incorporation rate of ^{13}C (from glucose) at the investigated temperatures (37 and 25°C) over time. Each point on the graphs is the mean of at least five replicates, and error bars on each time point indicate standard deviation.

Supplementary information

High performance liquid chromatography-evaporative light scattering detector

Method development and optimisation for HPLC-ELSD

Prior to measurement of the glucose content in bacterial supernatants, glucose standard stock solution (5 g/L) was prepared in de-ionised water using clean falcon tubes. Serial dilutions of glucose calibration standards at 10% v/v were prepared to mimic quantitative glucose levels as we have reported previously[6]. Reference glucose samples were then used to assess and validate the limit of detection (LOD), linearity and accuracy of experimental protocols. It is also worth mentioning that *E. coli* were grown in minimal medium with identical glucose concentration (at $t = 0$ h) as the prepared glucose stock solution (5 g/L).

Supernatants for *E. coli* cells harvested at five time points (*viz.* 0, 1, 2, 3 and 4 h) were centrifuged as already explained in the sample preparation section of the main article. Following this centrifugation process, supernatants were decanted into separate Falcon tubes. Both the supernatants and glucose standard solutions samples were filtered through sterile membrane filters with 0.2 μm pore size (Sigma Aldrich, UK) to remove bacterial cells/large biomolecules and any suspended solute impurities before HPLC-ELSD analysis.

HPLC-ELSD instrumentation and sample analysis

HPLC measurements were conducted using a HPLC Agilent 1260 Infinity II system equipped with a reversed-phase 4.6 x 100 mm Poroshell 120 EC–C18 column with 4 μm particle size and an evaporative light scattering detector (ELSD) (all from Agilent technologies, UK). The analytical method was run over 10 min with mobile phase in linear gradient mode consisting of 90% water held for 0.5 min followed by 100% acetonitrile for 5-6 min and finally 90% water for 6.10-10 min. The retention time and peak shapes on chromatograms for supernatants were compared with calibration curves for pure glucose aqueous solutions. For each sample, 10 μL were injected by an auto-injector, and all measurements were performed in triplicates (analytical replicates). The run time for each sample and standard solution was 10 min and samples were steadily pumped at 1.2 mL/min flow rate and column temperature set to 30°C. An ELSD was used for all chromatographic measurements. Peak areas for glucose standards and in supernatants were averaged and employed for quantitative analysis.

Results

Figure S6 below displays two time profiles representing the concentration (% v/v) of glucose in sample supernatants of *E. coli* collected at 0, 1, 2, 3 and 4 h after incubation at 37°C and 25°C. It can be clearly seen that cells grown under 37°C condition incorporated the ^{13}C heavy isotope more rapidly, and this was inversely proportional to the amount of ^{13}C-glucose remaining in supernatant at increasing sampling time points. This was consistent with OD_{600} measurements and kinetic characterisation of ^{13}C incorporation (Figures 3, 4 and S9). As expected this suggests that *E. coli* growing at 37°C exhibited much higher metabolic activity and ^{13}C assimilation than the cells incubated at 25°C, when the only variable changed was the temperature of growth, whilst all other experimental conditions were kept constant.

Supplementary information

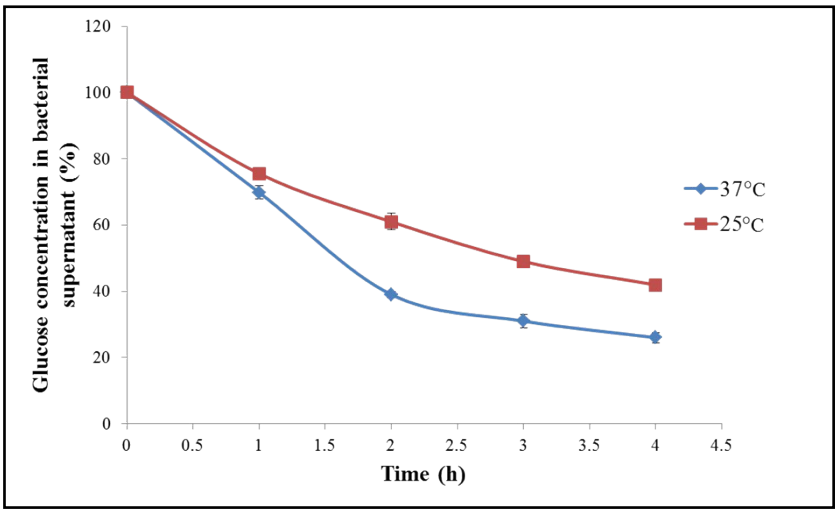

Figure S6. Levels of glucose in supernatants of *E. coli* cells incubated at 37°C (blue line) and 25°C (red line) quantified using HPLC-ELSD. Each point on the graphs represent mean peak area for glucose signals measured from 3 replicates for cells sampled at 0, 1, 2, 3 and 4 h. Error bars on each time point indicate standard deviation. The point at 0 h was before uptake of the glucose in the minimal medium (5 g/L).

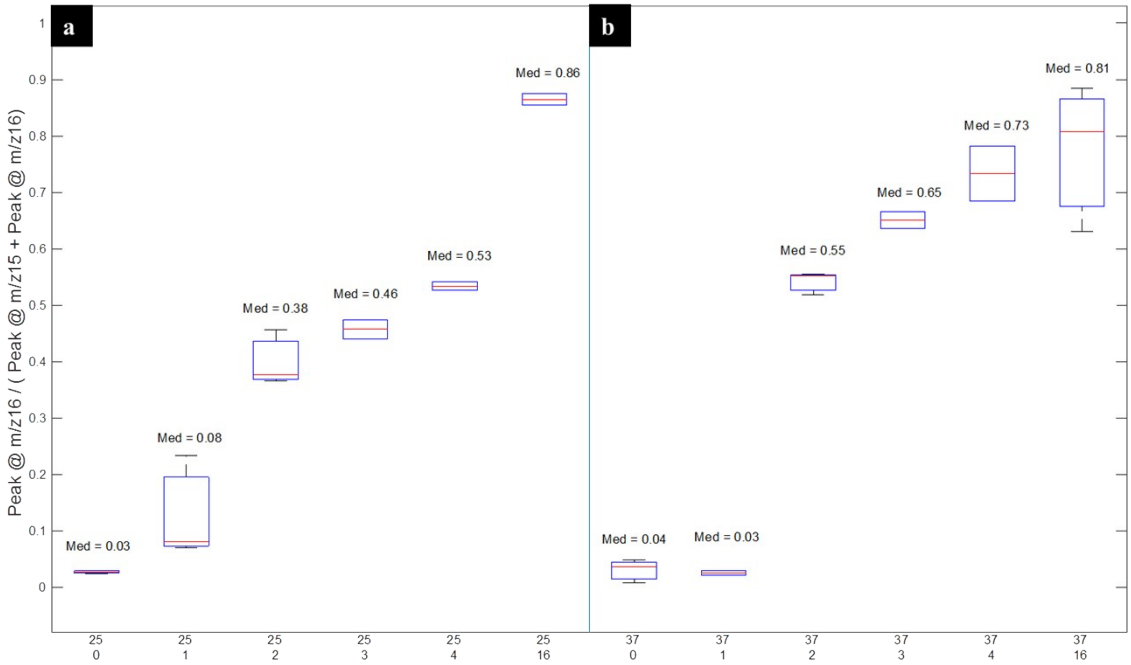

Figure S7. Plots from SIMS analysis of cells during ^{13}C incorporation illustrating quantitative detection of ^{13}C in *E. coli* incubated on ^{13}C-glucose collected at different time intervals under **(a)** 37°C and **(b)** 25°C. All analyses were performed from 3 independent biological x 3 technical replicates and the plots show box-whiskers where the red horizontal line is the median ratio, the top and bottom of the boxes are the 25th and 75th percentiles; the size of the box is the interquartile range (IQR); the whiskers extend to the most extreme data points which are not considered outliers, defined as no more than 1.5 × IQR outside of the IQR. The concentration of ^{13}C in cells increased with time at both temperatures, though ^{13}C enrichment by cells incubated at 37°C was generally faster. The numbers in the x-axis 25 and 37 represent cultivation temperatures in °C whereas the integers ranging from 0-4 and 16 underneath temperature values represent cultivation time of bacteria in hours.

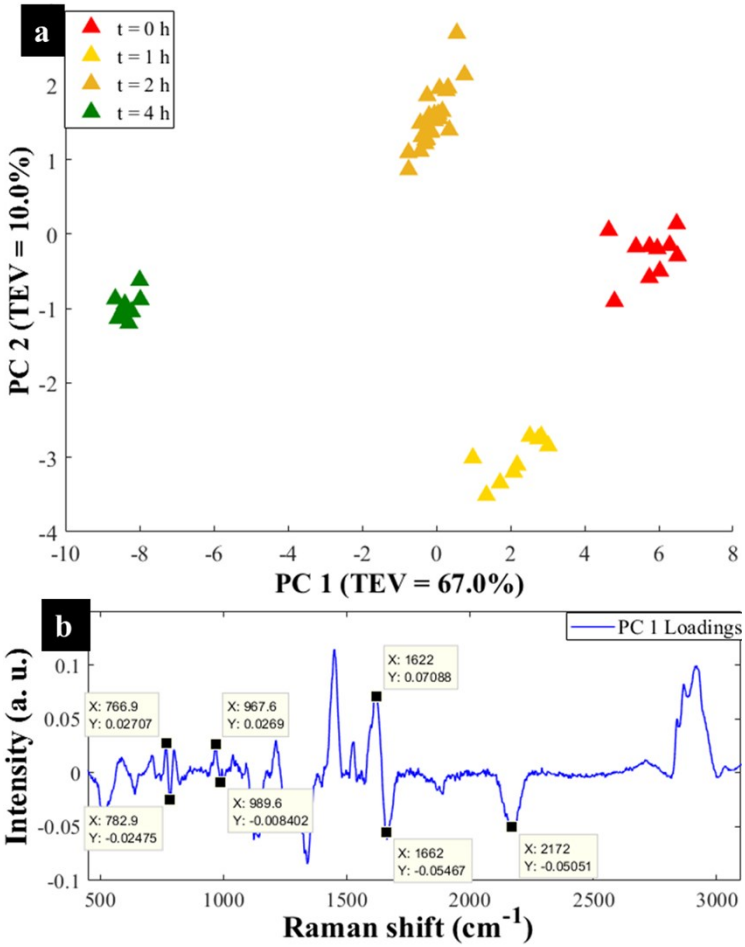

Figure S8. **(a)** PCA scores plot from pre-processed Raman data of initially ^{13}C-enriched *P. putida* undergoing reverse labelling from *P. putida-E.coli* co-culture in MMP (minimal medium supplemented with 0.2 g/L ^{12}C phenol) for 4 h. The trajectory from 0 to 4 h illustrates a time, D_2O and ^{12}C concentration-mediated clustering trend. **(b)** PC1 loadings clearly highlighting complete blueshift of bands for nucleobases (767→783 cm^{-1}) and amide I (1622→1661 cm^{-1}) after 4 h during reverse labelling. The Raman band for phenylalanine did not completely shift to its ^{12}C position in 4 h. The numbers on the PCA scores plot represent sampling time points for bacterial cells.

Supplementary information

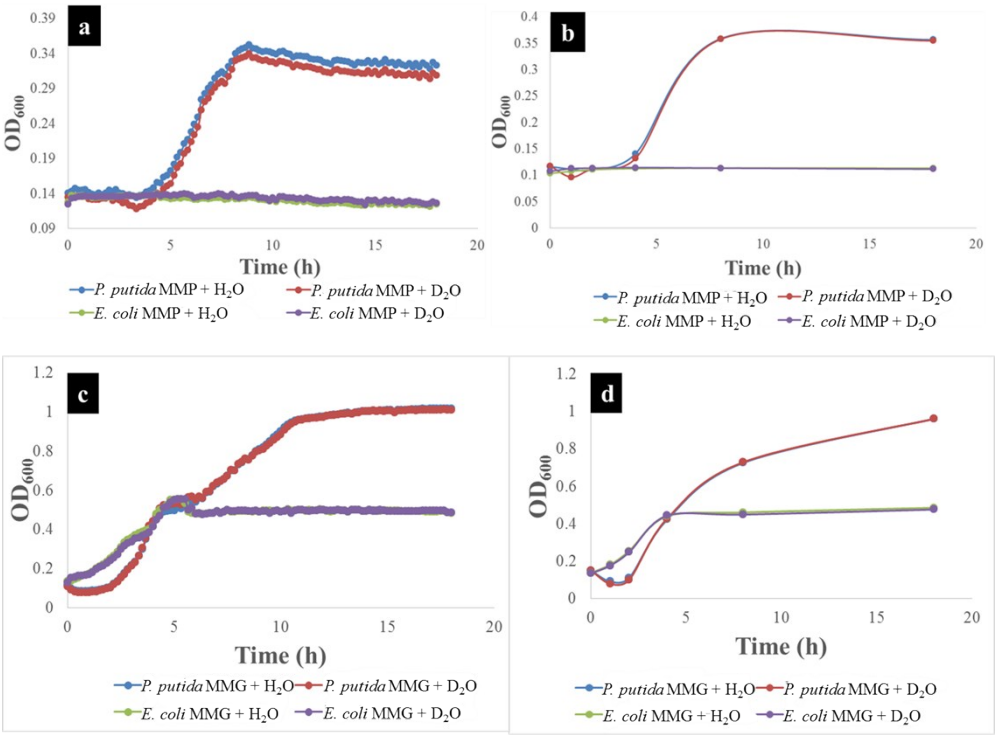

Figure S9. Averaged growth profiles for initially ^{13}C-enriched *P. putida* and *E. coli* cultivated in MMP (minimal medium and phenol) with or without 30% D_2O for 18 h as, **(a)** axenic and **(b)** co-cultures. The growth profiles for *P. putida* and *E. coli* in MMG (minimal medium and glucose) in the presence or absence of 30% D_2O **(c)** axenic and **(d)** co-cultures as controls. Whilst *P. putida* showed steady growth in both MMP and MMG growth conditions, *E. coli* cell density was unchanged in MMP **(a, b)** but grew normally in MMG control experiments **(c, d)** during 18 h of incubation.

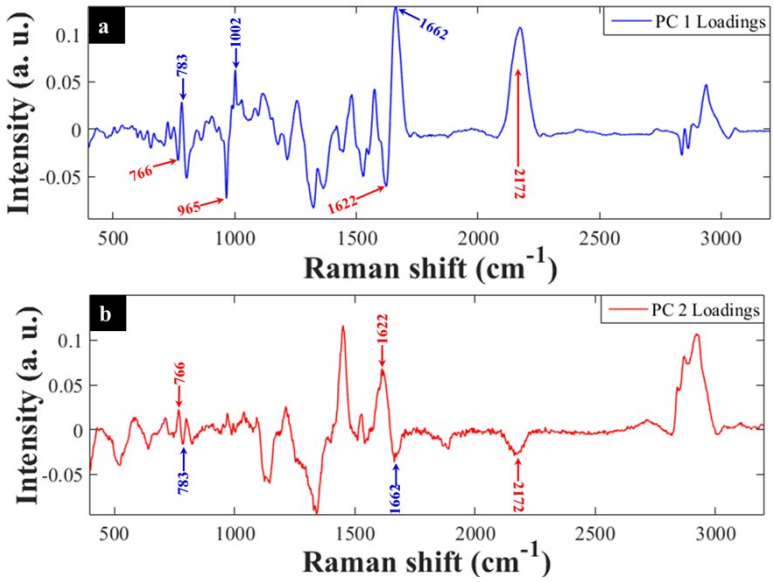

Figure S10. PC1 **(a)** and PC2 **(b)** loadings plot of initially ^{13}C-enriched *P. putida* from MMP with 30% D_2O co-culture indicating the main spectral inputs linked with PCA clustering patterns in Figure 6e during reverse labelling with ^{12}C from phenol. The arrows indicate the major peaks affected by ^{12}C and D_2O incorporation with red arrows representing ^{13}C positions (redshift) whilst blue arrows show ^{12}C Raman frequencies (blueshift) during reverse isotope uptake or no band shift.

Supplementary information

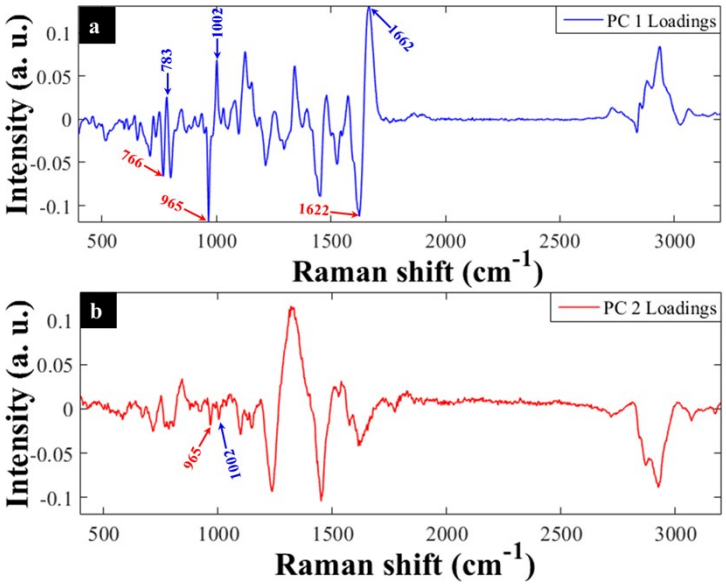

Figure S11. PC1 **(a)** and PC2 **(b)** loadings plot of initially ^{13}C-enriched *P. putida* in *P. putida-E. coli* co-culture under MMP with H_2O highlighting the major spectral variables responsible for PCA clustering distributions on Figure 6f during reverse ^{12}C assimilation event. The arrow heads indicate the major peaks affected by ^{12}C and D_2O consumption with red arrows representing ^{13}C positions (redshift) whilst blue arrows show ^{12}C positions during reverse labelling or no band shift.

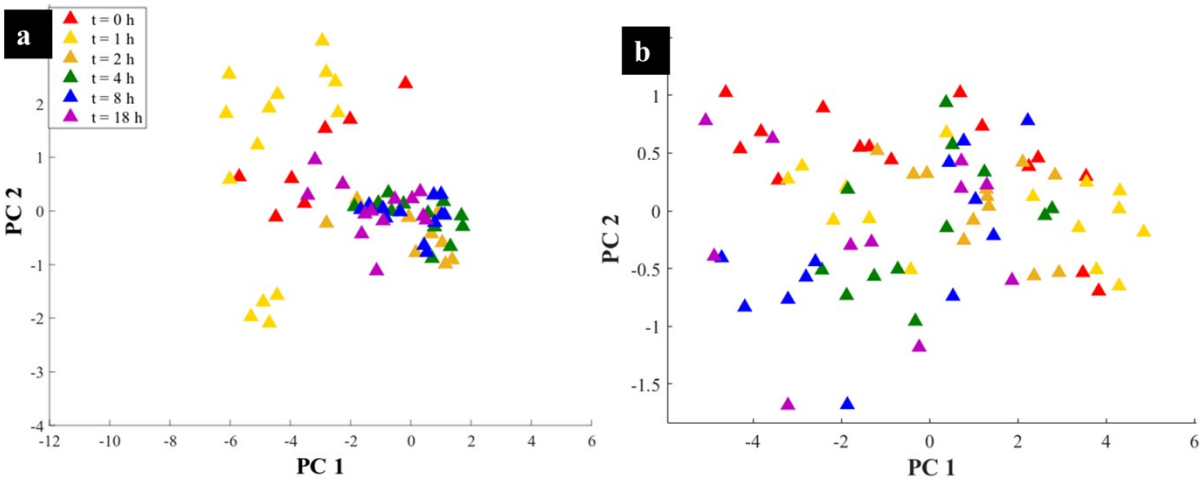

Figure S12. PCA scores for Raman data of initially ^{13}C-enriched *E. coli* mono culture in MMP with: **(a)** 30% D_2O and **(b)** H_2O. No recognisable biologically meaningful patterns were captured after 18 h of cell incubation.

Supplementary information

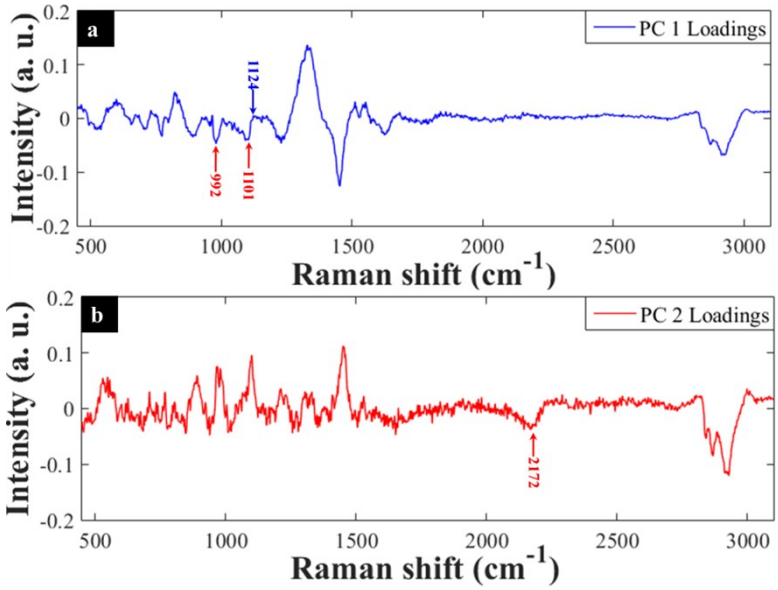

Figure S13. PC1 **(a)** and PC2 **(b)** loadings of initially ^{13}C-enriched *E. coli* from MMP with 30% D_2O co-culture. On PC1; during 18 h of growth, a peak appeared at 992 cm^{-1} when H at either ortho- or para-carbon position was substituted by D. A spectral redshift was also detected from 1124 to 1101 cm^{-1} due to D incorporation in lipids as shown on PC1 loadings **(a)**. A distinctive C–D band was detected along PC2 loadings **(b)**, which is consistent with Raman spectra (Figure 5c) and PCA (Figure 6g). No spectral blueshift due to ^{12}C rSIP during 18h of cell incubation. The arrow heads indicate the major peaks affected by D_2O labelling with red arrows representing ^{13}C positions (redshift) whilst blue arrows show standard Raman wavenumbers.

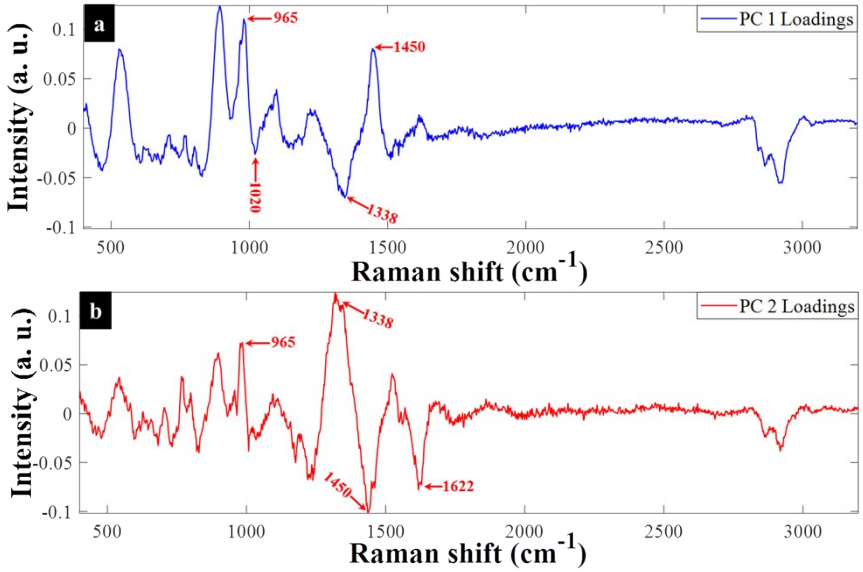

Figure S14. PC1 **(a)** and PC2 **(b)** loadings plot of initially ^{13}C-enriched *E. coli* from MMP with H_2O co-culture. During 18 h of bacterial growth, no blueshifts due to ^{12}C rSIP were detected. The C–D bands were not observed for bacteria cultivated in MMP with H_2O co-cultures. The red arrows indicate standard Raman bands, indicating intensity differences which were the basis of clustering on PCA in Figure 6h.

Reference

1. P. H. C. Eilers, *Anal. Chem.*, 2004, **76**, 404-411.
2. R. Bro and A. K. Smilde, *J. Chemometr.*, 2003, **17**, 16-33.
3. H. Martens, J. P. Nielsen and S. B. Engelsen, *Anal. Chem.*, 2003, **75**, 394-404.
4. M. Chisanga, H. Muhamadali, D. I. Ellis and R. Goodacre, *Appl. Sci.-Basel*, 2019, **9**, 1163-1186.
5. P. S. Gromski, H. Muhamadali, D. I. Ellis, Y. Xu, E. Correa, M. L. Turner and R. Goodacre, *Anal. Chim. Acta*, 2015, **879**, 10-23.
6. M. Chisanga, H. Muhamadali, R. Kimber and R. Goodacre, *Faraday Discuss.*, 2017, **205**, 331-343.